Applied Thermal Engineering 111 (2017) 60–67

Contents lists available at ScienceDirect

Applied Thermal Engineering

journal homepage: www.elsevier.com/locate/apthermeng

Research Paper

Thermodynamic analysis and optimization of a Stirling cycle for lunar surface nuclear power system

Senqing Fan, Minghai Li *, Sizhong Li, Tong Zhou, Yupeng Hu, Song Wu

Institute of Systems Engineering, China Academy of Engineering Physics, 621999 Mianyang, China

HIGHLIGHTS

- Lunar surface nuclear power system with Stirling cycle for energy conversion.
- A model with finite time thermodynamics to describe the system thermal efficiency.
- Higher hot side temperature not exceeds 1050 K increased thermal efficiency.
- Higher cold side temperature decreased thermal efficiency but improved heat rejection.
- Higher convection heat transfer coefficient improved the thermal efficiency.

ARTICLE INFO

Article history:
Received 25 May 2016
Revised 7 August 2016
Accepted 9 August 2016
Available online 9 August 2016

Keywords:
Thermodynamic analysis
Nuclear power system
Lunar surface
Stirling cycle
Lowest mass

ABSTRACT

A model for the description of the thermal efficiency of a lunar surface nuclear reactor power system with eight free piston Stirling engines to generate nominal electrical power of 100 kWe was developed. The heat loss of the hot heat pipes, finite rate heat transfer, regenerative heat loss, finite regeneration process time and conductive thermal bridging losses were considered. The results showed that the thermal efficiency increased and then decreased with the hot side temperature increase. The highest thermal efficiency was about 0.29 under the condition of the effectiveness of the regenerator being 0.9 and compression ratio being 2. Higher cold side temperature had bad effect on the thermal efficiency but could reduce the size of the heat rejection system. When the cold side temperature was designed as 500 K, the lowest power system mass of 6.6 ton could be obtained. Enhanced heat transfer of the heat exchangers would increase the thermal efficiency but higher values of the nominal convection heat transfer coefficient of the heat exchangers would lead to a negligible thermal efficiency increase. The results obtained here may provide a new ideal to design lunar surface nuclear powered Stirling cycle.

© 2016 Published by Elsevier Ltd.

1. Introduction

The earth's moon is a potential destination for future human space exploration and a wide range of activities including geological exploration, astronomical experiments, manufacturing and utilization of natural resources would be realized [1–4]. Many nations have expressed interest in sending crewed missions to the moon within the past few decades, with an eventual goal of establishing permanent outposts, requiring reliable and expandable electrical power of 10–100 s of kWe for many years and independent of the sun. The long lunar rotational period of about 28 days results in up to 2 weeks of darkness, depending on the selected site for the outpost on the lunar surface. Under this condition, the electrical power can be hardly met using the photovoltaic solar power system with nighttime energy storage or using the isotopic power. Nuclear fission reactor power system offers a low mass and compact alternative for mature lunar outpost and would generate steady electrical power continuously irrespective of the latitude of the outpost on the lunar surface and independent of the sun [5–7]. The essential components of the lunar surface nuclear power system are the reactor, the power conversion system and the heat rejection system [8–11].

The power conversion technologies for space nuclear power system are usually classified as the static and dynamic methods. Static conversion technologies of thermoelectric (TE), alkali-metal thermal-to-electric conversion (AMTEC) units and thermionic (TI), were inherently modular and load following, in addition to the absence of moving parts [8,12]. Despite the merits, the conversion efficiency was generally lower than 10% and therefore the

* Corresponding author at: Institute of Systems Engineering, China Academy of Engineering Physics, No. 64 Mianshan Road, Youxian District, 621999 Mianyang, China.
E-mail address: limh@caep.cn (M. Li).

http://dx.doi.org/10.1016/j.applthermaleng.2016.08.053
1359-4311/© 2016 Published by Elsevier Ltd.

Nomenclature

Q	heat (W or kW)
T	temperature (K)
h	heat transfer coefficient (W K^{-1} or W m^{-2} K^{-1})
k_0	heat leak coefficient (W K^{-1})
A	heat transfer area (m^2)
W	work (J)
P	power (W)
M	regenerative time constant (K s^{-1})
R	universal gas constant (J mol^{-1} K^{-1})

Greek symbols

Δ	regenerator loss
η	thermal efficiency
ξ	emissivity factor
ε	effectiveness
δ	Stefan-Boltzmann constant (W m^{-2} K^{-4})
λ	compression ratio

Subscripts

H	hot side
C	cold side
R	regenerator
L	loss
I	reactor
IN	fission heat
HP	heat pipes
HC	convective heat transfer at cold side
CC	convective heat transfer at cold side
s	nuclear power system
t	Stirling engine
0	ambient condition
1–4	process state

specific power of the system could hardly exceed 10 We/kg [3,8]. Dynamic energy conversion technologies of closed Brayton cycle (CBC) and Rankine cycle, typically generated high conversion efficiencies of between 20% and 30% [9,13]. Stirling engine is one of the most promising energy conversion technologies for space power system, since it results in high thermal efficiency and good reliability [14–16]. The Stirling engine can combines high energy conversion efficiency with high power output to system mass. In this study, the free-piston Stirling engines (FPSE) were used as the energy conversion units. The proposed lunar space nuclear power system with Stirling cycle for energy conversion is schematically described in Fig. 1. The nuclear fission heat generated in the reactor core with the temperature of about 1200 K is considered as the heat resource of the Stirling engine. Some of the heat would be lost through radiation during the heat transfer by the heat pipes owing to the high temperature. Part of the heat absorbed by the hot side heat exchanger of the Stirling engine is converted into electrical power and the exhaust heat is rejected from the cold side heat exchanger. A cooling loop can transport the exhaust heat to the heat rejection system and at last the exhaust heat is rejected to the outer space by the radiative heat transfer through the radiators.

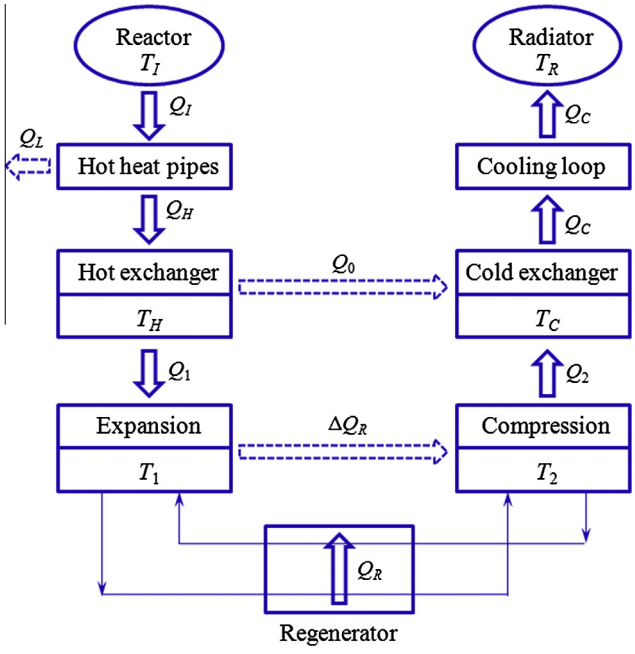

Fig. 1. Linear diagram of the lunar surface nuclear power system with Stirling cycle.

The radial cross-section view of the reactor is illustrated in Fig. 2. The reactor comprises 127 heat pipes and 342 fuel pins with UO_2. The reactor uses neutron Spectral Shift Absorber (SSA) additives in the fuel to satisfy the requirement of remaining the sufficiently subcritical in the unlikely event of a launch abort accident [6]. The ODS-MA956 steel encasement is made for the fuel pins frits, the core frits and the reactor vessel, owing to the high nominal exit temperature of the core [17]. The reactor core vessel is surrounded by a BeO radial reflector and the reflector is clad in thin stainless steel to protect from meteorites impact and prevent sublimation of BeO into space. The control of the reactor starting up, shutting down and operation through the end of life is accomplished using a total of six BeO/B_4C rotating drums in the radial reflector. The control drums are also clad in stainless steel and faces with B_4C segment (4 mm thick and 120 °C sectors) enriched in ^{10}B. The control drums in the BeO radial reflector would be rotated with the B_4C segments facing the core during launch before the reactor startup on the lunar surface.

The energy conversion is achieved in the Stirling engine, with the helium as the working fluid circulating in a closed system. Eight Stirling engines are use as the energy conversion units for the lunar surface unclear power system with nominal electrical power of 100 kWe. The schematic diagram of the Stirling engine is illustrated in Fig. 3. The diameter and length (including no electrical motor) of one Stirling engine are 500 mm and 1000 mm, respectively. A Stirling engine configuration consists of a cylinder (contained with hot space and cold space), the hot side heat exchanger, the cold side heat exchanger, the regenerator, the power piston and the displacer piston. A Stirling cycle consists of four steps, including two isothermal and two isochoric steps [14,18–20]. The compression and expansion steps of the cycle takes place in the cylinder with the power piston at constant temperature [21]. The displacer piston shuttles the helium back and forth through the hot side heat exchanger, regenerator and cold side heat exchanger at a constant volume [22]. If the regenerator is ideal, the heat absorbed by the regenerator when the helium flows from the hot space to the cold space should be equal to the heat rejected from the regenerator when the helium flows from the cold space to the hot space [19]. However, the ideal regenerator requires an infinite area or infinite regeneration time to transfer

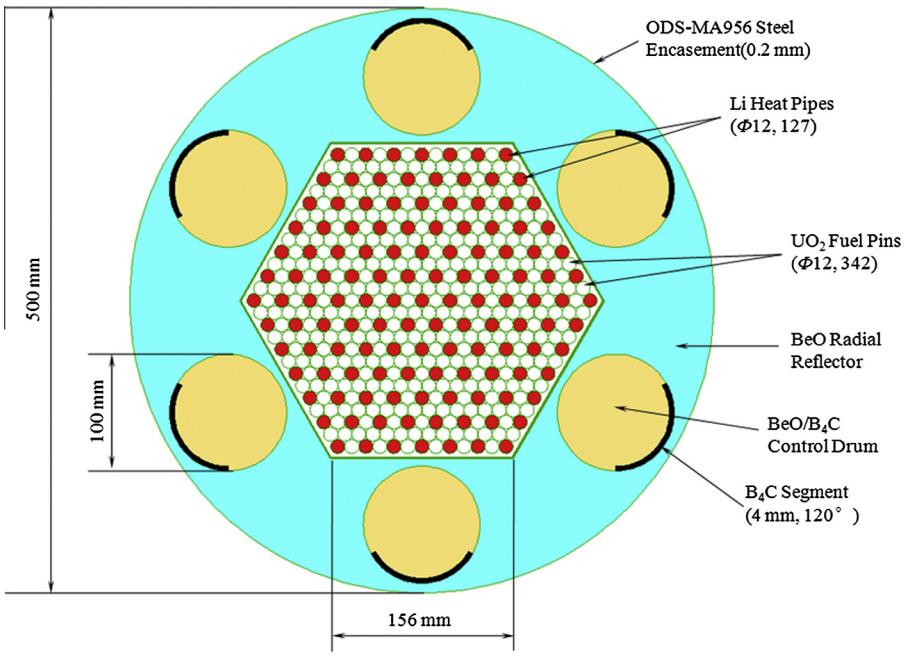

Fig. 2. Radial cross-sectional view of the lithium heat pipes disposal inside the nuclear reactor core.

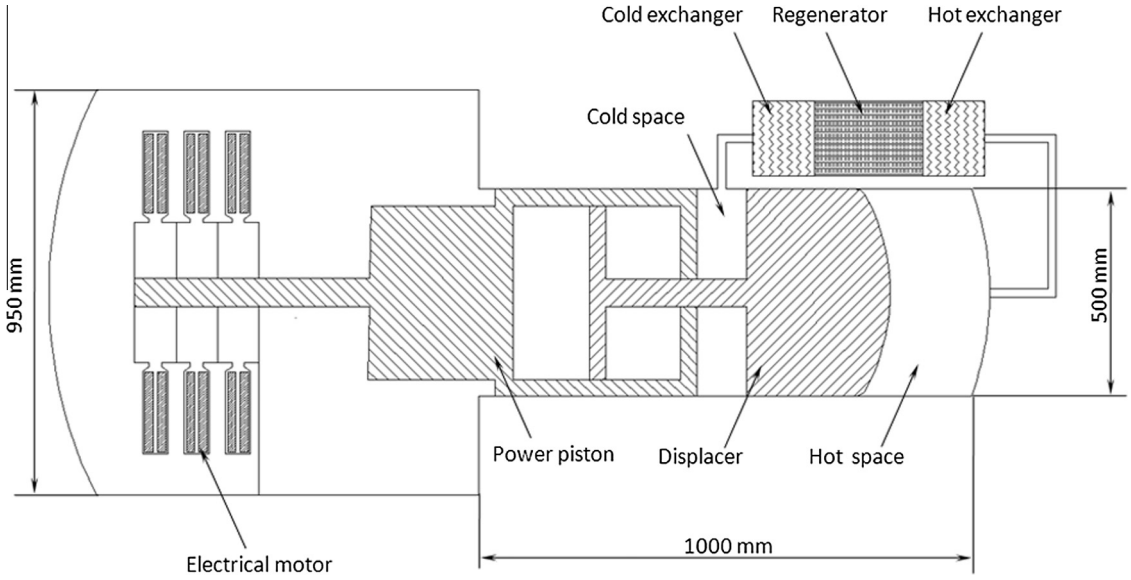

Fig. 3. A schematic diagram of a Stirling engine applied for the power system.

finite heat amount, which is impractical [18,23,24]. In a real Stirling cycle, a heat transfer loss would occur in the regenerator and a conductive thermal bridging loss would also occur between the hot side and cold side of the Stirling engine. Therefore, the energy conversion efficiency of the Stirling cycle is still much lower than that of the Carnot cycle [25,26].

In recent years, several researchers have paid attention to the thermal efficiency of solar-powered Stirling heat engine with finite time thermodynamics and some of the achievements may provide good ideals for the Stirling cycle applied for lunar surface nuclear power system [22,27]. To the authors' knowledge, there has been no work undertaken to describe the thermal efficiency of the Stirling cycle applied for lunar surface nuclear power system. It should be noted that nuclear power systems turned into lunar surface electrical propulsion differed strongly from usual ground-based power systems regarding the importance of overall size and mass. Large size and mass could increase the difficulty of the power system launch and cause several problems during the operation of the power system or increase the system's cost. The aim of this study is to develop a model based on the finite time thermodynamics to describe the thermal efficiency of the lunar surface nuclear power system with Stirling cycle, explore the effect of the designed parameters on the thermal efficiency, size and mass of the power system.

2. Thermal efficiency model of the power system

A schematic illustration of the various heat flows and losses that are included in the presented model is presented in Fig. 4. The processes of a–b and c–d work at constant temperatures T_1 and T_2,

respectively. The processes of b–c and d–a work at constants volumes V_1 and V_2, respectively. Some of the heat absorbed is converted into power output W. There is a conductive heat transfer occurring, namely conductive thermal bridge loss or heat leak Q_0, when heat Q_1 is released to the process of a-b. In addition, heat loss ΔQ_R should be taken into account, when regenerative heat Q_R is transferred from the b–c to the d–a.

In order to develop a simple and validating model for the thermal efficiency of the power system with Stirling engine, the following considerations are assumed:

- Radiation is the only heat loss during heat transfer from the reactor to the Stirling engine.
- Conduction leads to the heat loss between the hot side and the cold side.
- The specific heat of working fluid does not change with temperature.
- The heat transfer coefficients and working fluid velocity are constant with time and space.
- The working fluid obeys perfect gas law.
- There is no temperature gradient in the heat exchangers.

2.1. Thermal efficiency of the hot heat pipes

Considering the heat loss of the hot heat pipes by radiation, owing to the high temperature of the hot heat pipes, the energy balance equation and thermal efficiency of the hot heat pipes would be described as follows:

$$Q_{IN} = Q_L + Q_H = \xi\delta A\left(T_H^4 - T_0^4\right)\tau + h_{HP}A(T_I - T_H)\tau \tag{1}$$

and

$$\eta_{HP} = \frac{h_{HP}A(T_I - T_H)\tau}{Q_{IN}} = \frac{h_{HP}(T_I - T_H)}{\xi\delta\left(T_H^4 - T_0^4\right) + h_{HP}(T_I - T_H)} \tag{2}$$

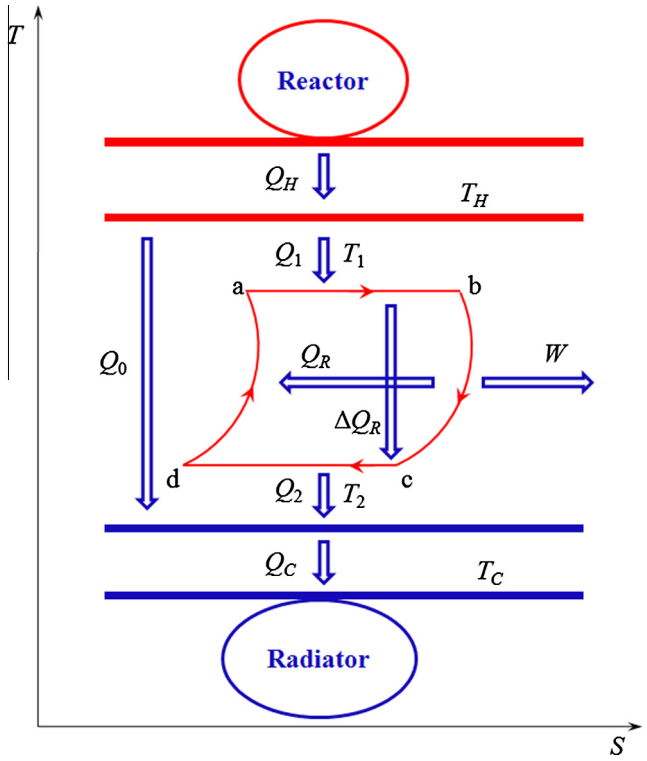

Fig. 4. A schematic illustration of the various heat flows and losses that are included in the presented model.

where Q_{IN}, Q_L and Q_H are the fission heat generated from the reactor, heat loss of the hot heat pipes and heat absorbed by the hot side heat exchanger; η_{HP} is the thermal efficiency of the hot heat pipes; A is the heat transfer area of the heat pipes T_I, T_H, T_0 are temperatures of the reactor, hot side heat exchanger and heat sink, respectively; ξ is the emissivity factor of the hot heat pipes; δ is the Stefan-Boltzmann constant; τ is the cycle period.

2.2. Thermal efficiency of the Stirling engine

The conductive thermal bridging losses (Q_0) from the hot side heat exchanger at temperature T_H to the cold side heat exchanger at temperature T_C is assumed to be proportional to the cycle time, which can be described as follows [23]:

$$Q_0 = k_0\tau(T_H - T_C) \tag{3}$$

where k_0 is the heat leak coefficient between the hot side and cold side heat exchangers.

It should be noted that there is a finite heat transfer rate in the regenerator and the regenerative heat transfer (Q_R) can be described as follows [28]:

$$Q_R = nC_p\varepsilon_R(T_1 - T_2) \tag{4}$$

where n is the molar number of the working fluid; C_p is the molar specific heat of the working fluid in the regenerative process; ε_R is the effectiveness of the regenerator.

The heat loss (ΔQ_R) during two regenerative processes per cycle can be calculated as follows [18,19,23]:

$$\Delta Q_R = nC_p(1 - \varepsilon_R)(T_1 - T_2) \tag{5}$$

The time of the regenerative processes is not negligible owing to the influence of irreversibility of the finite rate heat transfer. Using a regenerative time constant to determine the time needed for the displacement phases may be a typical approach in so-called finite time thermodynamics. In order to calculate the time of the regenerative processes, the temperature of the working fluid in the regenerative processes as a function of time is described as follows [18,19,23]:

$$\frac{dT}{dt} = \pm M_i \tag{6}$$

where M is the proportional constant independent of the temperature difference and dependent only on the property of the regenerative material, called regenerative time constant and the ±sign belong to the heating ($i = 1$) and cooling ($i = 2$) processes, respectively. The choice of the regenerator material and its dimensions are important optimization options in the design of a Stirling machine. In this research, the matrix of packed balls or wire mesh would be used for the regenerator. It is necessary to expose the maximum surface area of matrix so that matrix should be finely divided, in order to improve heat transfer coefficient and to establish the minimum temperature difference between matrix and the fluid.

The time of the two isochoric processes can be obtained as follows [18,19,23]:

$$t_3 = \frac{T_1 - T_2}{M_1} \tag{7}$$

$$t_4 = \frac{T_1 - T_2}{M_2} \tag{8}$$

The heat transfer between the hot side heat exchanger at temperature T_H and the working fluid at temperature T_1 obeys convection law. The amount of heat absorbed by the working fluid from the hot side heat exchanger can be described as follows [18,19,23]:

$$Q_1 = h_{HC}(T_H - T_1)t_1 = nRT_1\ln\lambda + nC_p(1 - \varepsilon_R)(T_1 - T_2) \tag{9}$$

Convection heat transfer is assumed to be the main mode of heat transfer between the working fluid at temperature T_2 and cold side heat exchanger at temperature T_C. The amount of heat released by the working fluid to the cold side heat exchanger can be described as follows:

$$Q_2 = [h_{CC}(T_2 - T_C)]t_2 = nRT_2 \ln\lambda + nC_p(1-\varepsilon_R)(T_1 - T_2) \tag{10}$$

where Q_1 is the amount of heat absorbed by the working fluid; Q_2 is the amount of heat released by the working fluid; h_{HC} is the nominal convection heat transfer coefficient of the hot side heat exchanger; h_{CC} is the nominal convection heat transfer coefficient of the cold side heat exchanger; R is the universal gas constant and λ is the compression ratio during the regenerative processes, which could be expressed as the volume ratio (including no dead volumes):

$$\lambda = \frac{V_1}{V_2} \tag{11}$$

According to Fig. 4 and the major irreversibility mentioned above (finite rate heat transfer, regenerative heat loss, finite regeneration process time and conductive thermal bridging losses), the net heat absorbed by the hot side heat exchanger can be described as follows:

$$Q_H = Q_1 + Q_0 \tag{12}$$

The net heat released by the cold side heat exchanger can be described as follows:

$$Q_C = Q_2 + Q_0 \tag{13}$$

The cyclic period (τ) can be obtained by combining Eqs. (7)–(10), described as follows:

$$\begin{aligned}\tau &= t_1 + t_2 + t_3 + t_4 \\ &= \frac{nRT_1\ln\lambda + nC_p(1-\varepsilon_R)(T_1-T_2)}{h_{HC}(T_H - T_1)} + \frac{nRT_2\ln\lambda + nC_p(1-\varepsilon_R)(T_1-T_2)}{h_{CC}(T_2-T_C)} \\ &\quad + (T_1 - T_2)\left(\frac{1}{M_1} + \frac{1}{M_2}\right)\end{aligned} \tag{14}$$

Considering the cyclic period of the Stirling engine, the power output (P) and thermal efficiency (η_t) of the engine can be described as follows:

$$P = \frac{W}{\tau} = \frac{Q_H - Q_C}{\tau} \tag{15}$$

$$\eta_t = \frac{Q_H - Q_C}{Q_H} \tag{16}$$

Combining Eqs. (9)–(16) leads to the following expressions for the power output and thermal efficiency of the Stirling engine:

$$P = \frac{T_1 - T_2}{\frac{T_1 + a(T_1-T_2)}{h_{HC}(T_H - T_1)} + \frac{T_2 + a(T_1-T_2)}{h_{CC}(T_2 - T_C)} + F_1(T_1 - T_2)} \tag{17}$$

$$\eta_t = \frac{T_1 - T_2}{T_1 + a(T_1-T_2) + [k_0(T_H - T_C)]\left[\frac{T_1 + a(T_1-T_2)}{h_{HC}(T_H-T_1)} + \frac{T_2 + a(T_1-T_2)}{h_{CC}(T_2-T_C)} + F_1(T_1-T_2)\right]} \tag{18}$$

where

$$a = \frac{C_p(1-\varepsilon_R)}{R\ln\lambda} \tag{19}$$

$$F_1 = \frac{1}{nR\ln\lambda}\left(\frac{1}{M_1} + \frac{1}{M_2}\right) \tag{20}$$

The power output and thermal efficiency of the Stirling engine are maximized simultaneously. In order to maximize the power output, take the derivative of the Eq. (17) with respect to the decision variables and equate it to zero. Then, solving the decision variables and substituting the values to Eqs. (17) and (18) can give the maximum power output and the optimal efficiency of the Stirling engine.

The thermal efficiency of the nuclear power system is equal to product of the thermal efficiency of the hot heat pipes and the thermal efficiency of the Stirling engine. Therefore, the thermal efficiency (η_s) of the nuclear power system can be described as follows:

$$\begin{aligned}\eta_s &= \eta_{HP}\eta_t \\ &= \left[\frac{h_{HP}(T_I - T_H)}{\xi\delta\left(T_H^4 - T_0^4\right) + h_{HP}(T_I - T_H)}\right]\frac{1-\chi}{1 + a(1-\chi) + [k_0(T_H - T_C)]\left[\frac{1+a(1-\chi)}{h_{HC}(T_H-T_1)} + \frac{\chi + a(1-\chi)}{h_{CC}(\chi T_1 - T_C)} + F_1(1-\chi)\right]}\end{aligned} \tag{21}$$

where $\chi = T_2/T_1$.

3. Results and discussion

In order to investigate the optimum performance characteristics of the lunar surface nuclear power system conveniently and be consistent with previous works, the other parameters should be kept constant as $\chi = 0.5$, $h_{HC} = h_{CC} = 200\ \mathrm{W\ K^{-1}}$, $h_{HP} = 5000\ \mathrm{W\ m^{-2}\ K^{-1}}$, $n = 1$ mol, $\lambda = 2$, $\varepsilon_R = 0.9$, $\xi = 0.9$, $R = 8.314\ \mathrm{J\ mol^{-1}\ K^{-1}}$, $k_0 = 2.5\ \mathrm{W\ K^{-1}}$, $C_p = 15\ \mathrm{J\ mol^{-1}\ K^{-1}}$, $\delta = 5.67 \times 10^{-8}\ \mathrm{W\ m^{-2}\ K^{-4}}$, $T_I = 1200$ K, $T_H = 1000$ K, $T_C = 500$ K, $T_0 = 300$ K, $(1/M_1 + 1/M_2) = 2 \times 10^{-5}\ \mathrm{s\ K^{-1}}$ [19,23].

3.1. Effect of the hot side temperature

During the design of lunar surface nuclear power system, a surface temperature (T_I) of 1200 K was considered for the nuclear reactor core. The temperature of the hot side heat exchanger could be lower than that of the core temperature owing to the heat resistance of the heat pipes. The effect of hot side temperature on system thermal efficiency was illustrated in Figs. 5 and 6. It could be seen that the thermal efficiency increased slightly with the increase of hot side temperature. The peak values of the thermal efficiency could be obtained when the hot side temperature was about 1050 K. The thermal efficiency could decrease, if the hot side temperature increased continuously. It could be calculated that the thermal efficiency would decrease about 25%, when the hot side temperature increased from 1050 K to 1150 K. The decrease of the thermal efficiency of the hot heat pipes could account for this phenomenon. It could be calculated from Eq. (2) that the thermal efficiency of the hot heat pipes decreased with the increase of

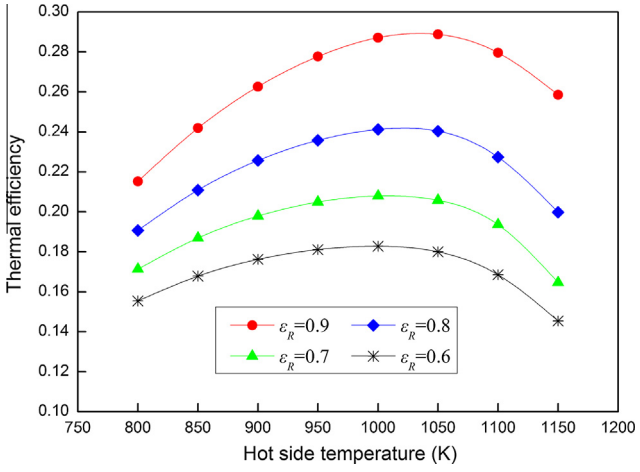

Fig. 5. Effect of the hot side temperature and effectiveness of the regenerator on the system efficiency.

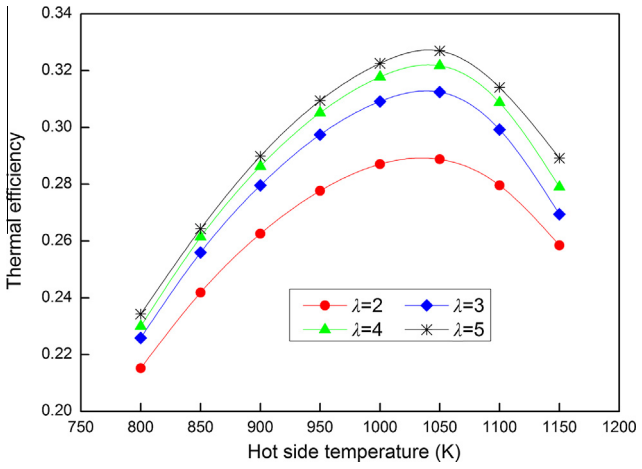

Fig. 6. Effect of the hot side temperature and volume ratio on the system efficiency.

the hot side temperature, owing to the heat loss by radiation. When the hot side temperature increased from 1050 K to 1150 K, the thermal efficiency of the hot heat pipes could decrease from 0.90 to 0.78. How to reduce the heat loss of the hot heat pipes would be a key issue for the nuclear power system. Besides, according to the exergy theory it could be known that the temperature difference between the reactor core and hot side heat exchanger could reduce the energy availability of the nuclear power system owing to the heat resistance of the heat pipes, even though it was expected to be no heat loss during the heat transfer process. Enhanced heat transfer between the reactor core and hot side exchanger would be a reasonable approach to increase the energy availability of the system. However, enhanced heat transfer was usually accomplished at the expense of the complexity and redundancy of the system, decreasing the system reliability. Therefore, extensive researches should be emphasized on the trade-off between the good thermal performance and the reliability of the system. It could be seen from Fig. 6 that higher thermal efficiency of could be obtained if the compression ratio was higher. However, higher compression ratio would be limited by the practical application, since compression ratios above 2 are rather unrealistic in Stirling engines. Therefore, the compression ratio of the Stirling engine would be kept about 2, during the design of the nuclear power system.

The thermal power generated in reactor core should be 500 kWt to match the nominal electrical power of 100 kWe, if the thermal efficiency of the system was assumed as 0.2. The electrical power output under different conditions was illustrated in Table 1. It could be seen that the thermal power can be kept lower than 500 kWt at any temperature within the scope when the effectiveness of the regenerator was higher than 0.8, since the electrical power was higher than 100 kWe. However, when the effectiveness of the regenerator was lower than 0.7, 500 kWt of the thermal power can hardly generate 100 kWe of electrical power. In this case, higher thermal power was required and then high amount of exhaust heat was needed to be rejected, which could increase the size of the heat rejection and mass of the power system. Therefore, the most efficient and cost effective regenerator should be used for the Stirling engine.

Table 1
Electrical power output at different hot side temperatures and regenerator effectiveness.

Effectiveness	Electrical power output (kWe)			
(λ = 2)	T_H = 800 K	T_H = 900 K	T_H = 1000 K	T_H = 1100 K
0.9	107	131	143	139
0.8	95	112	120	113
0.7	86	99	104	97
0.6	78	88	91	84

3.2. Effect of the cold side temperature

The effect of the cold side temperature on the thermal efficiency was illustrated in Figs. 7 and 8. It could be seen that higher cold side temperature would lead to lower thermal efficiency, which was consistent with the Carnot theory. It could be calculated that the thermal efficiency could decrease as much as 23%, when the cold side temperature increased from 400 K to 500 K. Higher thermal efficiency could be achieved by decreasing the cold side temperature, which would reduce the amount of heat to be radiated away and reduce the mass of the reactor. But lower cold side temperature could have bad effect on heat transfer through the radiator, leading to the increase of the size and mass of the radiator, since radiation heat transfer was greatly dependent on the cold side temperature. These factors led to an inverse and competing relationship between thermal efficiency and cold side temperature, which in turn impacted the size and mass of the heat rejection sys-

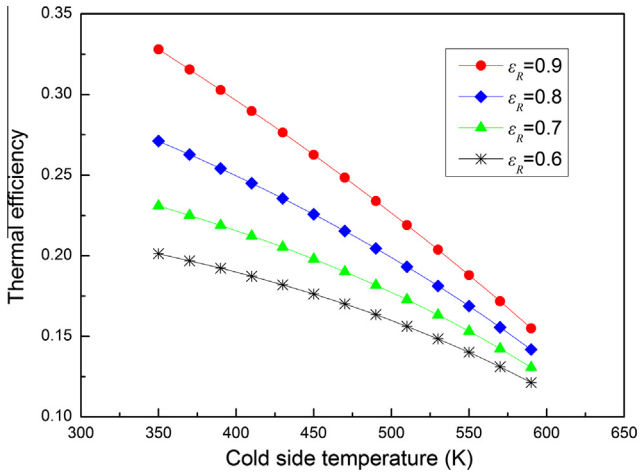

Fig. 7. Effect of the cold side temperature and effectiveness of the regenerator on the system efficiency.

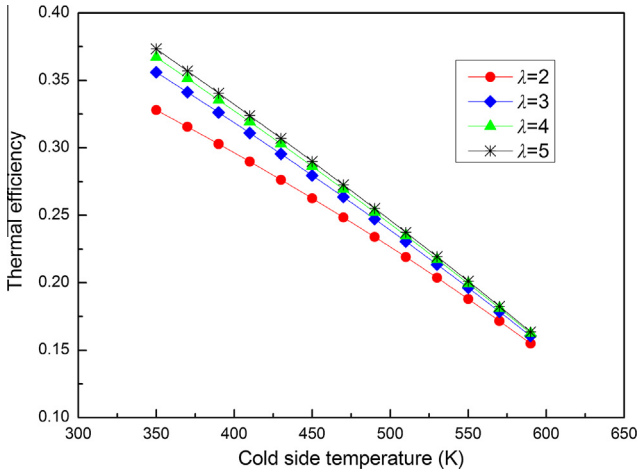

Fig. 8. Effect of the cold side temperature and volume ratio on the system efficiency.

Table 2
Size of the heat rejection system at different cold side temperatures.

Cold side temperature (K)	Rejection system size (m^2)
450	305
500	180
550	116

tem. According to the others' researches, the radiator was the largest component of the nuclear power system and the heat rejection system mass was a significant and often dominant portion of the overall nuclear power system mass [13]. Large radiator size and mass could increase the difficulty of the power system launch and cause several problems during the operation of the power system. Therefore, design trades were required to minimize the total mass based on the relative masses of the reactor and heat rejection system. Besides, the temperature of the heat sink could reach about 400 K, since the temperature of the heat sink would be changed during the whole operation period. If the cold side temperature was low, there would be some difficulty for the waste heat being rejected to the outer space.

The size of the rejection system at different cold side temperatures was illustrated in Table 2, which was calculated by the Stefan-Boltzmann radiation law. It could be seen that higher cold side temperature can greatly reduce the rejection system size. When the cold side temperature was increased from 450 to 550 K, the size could be reduced by 62%. However, the effect of the cold side temperature on the power system mass was not similar to that on the size. During the design of the lunar surface nuclear power system, it was expected to gain the lowest total mass under the premise of guaranteed electrical power supply. The mass of the power system could be easily obtained if the specific masses of the reactor, Stirling engine and heat rejection system were specified. According to the rich experiences of the China Academy of Engineering Physics, the required mass of the reactor and Stirling engine were assumed as 5.82 kg/kWt and 2.56 kg/kWt, respectively. The heat rejection mass was greatly dependent on the detailed designed parameters and we just reported the calculation results of the heat rejection mass in this research. The detailed design of the heat rejection system would be revealed in another research. The mass of the reactor, Stirling engine and heat rejection system were illustrated in Fig. 9. It could be seen that when the cooling temperature was at 450 K, the total mass was higher than 7.0 ton, since low cooling temperature leads to low heat rejection driven force and therefore larger mass of the heat rejection system was needed. When the cooling temperature was at 550 K, the total mass was still higher than 7.0 ton, since higher cooling temperature leads to low thermal efficiency and larger masses of the reactor and Stirling engine were needed. When the cooling temperature was at 500 K, the low total mass could be obtained, which was about 6.6 ton, with the specific mass of the power system being 66 kg/kWe.

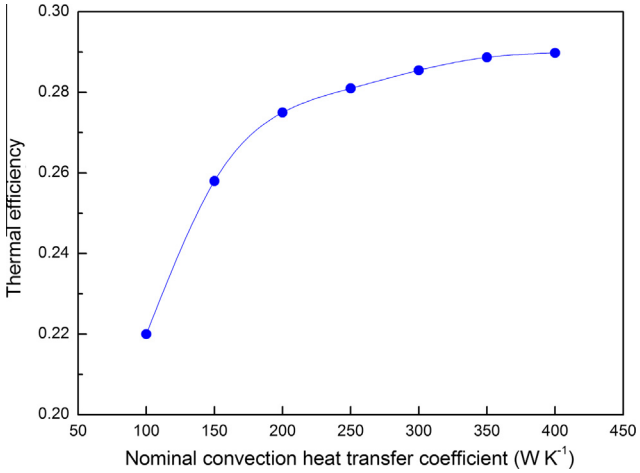

Fig. 10. Effect of the nominal convection heat transfer coefficient of the hot side heat exchanger on the system efficiency.

3.3. Effect of the nominal convection heat transfer coefficient

The effect of the nominal convection heat transfer coefficient of the hot side heat exchanger on the thermal efficiency was illustrated in Fig. 10. It could be seen that an increase of the convection heat transfer coefficient resulted in an increase of the thermal efficiency of the nuclear power system. Moreover, the thermal efficiency increased asymptotically and reached a maximum value of 0.29 for the range of the nominal convection heat transfer coefficient. It could be deduced from Fig. 10 that the design of a hot side heat exchanger with the convection heat transfer coefficient higher than 300 W K^{-1} would not bring worthy results, since a slightly increase of thermal efficiency may come at the expense of great mass changes of the system [13]. The effect of the nominal convection heat transfer coefficient of the cold side heat exchanger

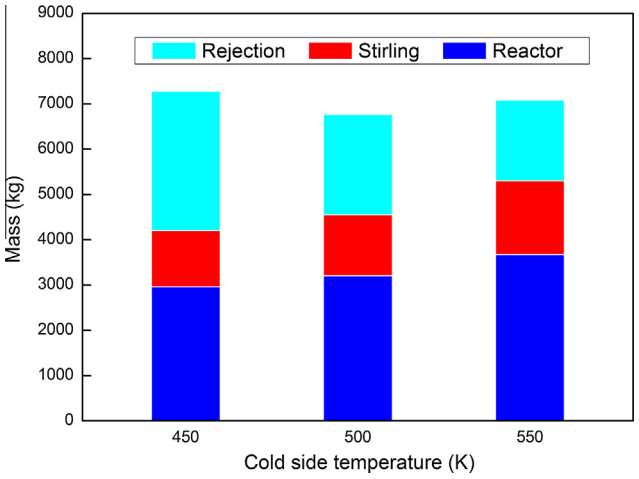

Fig. 9. Mass of the lunar surface nuclear power system at different cold side temperatures.

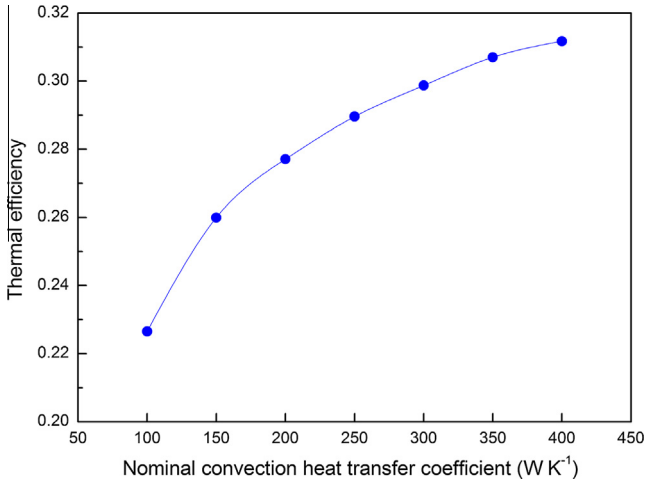

Fig. 11. Effect of the nominal convection heat transfer coefficient of the cold side heat exchanger on the system efficiency.

on the system efficiency was illustrated in Fig. 11. Likewise the nominal convection heat transfer coefficient of the hot side heat exchanger, an increase of the nominal convection heat transfer coefficient of the cold side heat exchanger provided an increase of the thermal efficiency. However, higher values of nominal convection heat transfer coefficient of the cold side heat exchanger still resulted in a negligible increase of the thermal efficiency. Therefore, a compromise between cold side heat exchanger mass and thermal efficiency should be also achieved in the system conception phase, although the detailed design of the heat exchanger was beyond the scope of this research. Comparing Figs. 10 and 11, it could be seen that higher thermal efficiencies would be achievable when the cold side heat exchanger was favored with nominal convection heat transfer coefficient increase. Changes in the nominal convection heat transfer coefficient of the hot side heat exchanger resulted in a maximum thermal efficiency of about 0.29, while this value could be reached about 0.31, varying the nominal convection heat transfer coefficient of the cold side heat exchanger. Furthermore, higher nominal convection heat transfer coefficient of the cold side heat exchanger could result in higher temperature of the radiator, which was great important for heat rejection to the outer space and would result in less size and mass of the radiator.

4. Conclusions

A theoretical model was developed for the thermal efficiency predication of a Stirling cycle applied for lunar surface nuclear power system. It was found that the maximum of the thermal efficiency of about 0.29 could be obtained, when the hot side temperature was 1050 K. The radiation heat loss of the hot heat pipes could lead to the decrease of the thermal efficiency if the hot side temperature was higher. A decrease of the cold side temperature could result in an increase of the thermal efficiency. But lower cold side temperature would have bad effect on heat rejection to the outer space by radiation, which could lead to a larger system size and mass. When the cold side temperature was 500 K, the lowest mass of the power system of 6.6 ton can be obtained. Higher nominal convection heat transfer coefficient of the heat exchangers could improve the system thermal efficiency. A compromise between heat exchangers' mass and system thermal efficiency should be considered, since higher values of nominal convection heat transfer coefficient of the heat exchangers resulted in a negligible increase of the thermal efficiency. In the future, more detailed description about the heat exchangers, Stirling engines and heat rejection system should be revealed.

Acknowledgements

The authors gratefully acknowledged the supports from the project "Innovation Fund of Institute of Systems Engineering of China Academy of Engineering Physics (No. 15cxj45)".

References

[1] T.M. Schriener, M.S. El-Genk, Neutronics and thermal–hydraulics analysis of a liquid metal fast reactor for expandable lunar surface power, Ann. Nucl. Energy 41 (2012) 48–60.
[2] M.S. El-Genk, T.M. Schriener, Long operation life reactor for lunar surface power, Nucl. Eng. Des. 241 (2011) 2339–2352.
[3] M.S. El-Genk, Space reactor power systems with no single point failures, Nucl. Eng. Des. 238 (2008) 2245–2255.
[4] E.V. Voevodina, V.M. Martishin, V.A. Ivanovsky, N.O. Prasolova, Shadow radiation shield required thickness estimation for space nuclear power units, Phys. Procedia 74 (2015) 158–164.
[5] L. Popa-Simil, Advanced space nuclear reactors from fiction to reality, Phys. Procedia 20 (2011) 270–292.
[6] L. Popa-Simil, Micro-structured nuclear fuel and novel nuclear reactor concepts for advanced power production, Prog. Nucl. Energy 50 (2008) 539–548.
[7] J. Alvarez-Ramirez, H. Puebla, G. Espinosa, A cascade control strategy for a space nuclear reactor system, Ann. Nucl. Energy 28 (2001) 93–112.
[8] M.S. El-Genk, Space nuclear reactor power system concepts with static and dynamic energy conversion, Energy Convers. Manage 49 (2008) 402–411.
[9] M.S. El-Genk, J.-M.P. Tournier, B.M. Gallo, Dynamic simulation of a space reactor system with closed Brayton cycle loops, J. Propul. Power 26 (2010) 394–406.
[10] J. Tarlecki, N. Lior, N. Zhang, Analysis of thermal cycles and working fluids for power generation in space, Energy Convers. Manage 48 (2007) 2864–2878.
[11] A.G. Yuferov, V.A. Linnik, M.A. Nikolaev, Parametric analysis of space nuclear power plants in thermodynamic design variables, Nucl. Energy Technol. (2016).
[12] D.M. Rowe, Applications of nuclear-powered thermoelectric generators in space, Appl. Energy 40 (1991) 241–271.
[13] G.B. Ribeiro, F.A.B. Filho, L.N.F. Guimarães, Thermodynamic analysis and optimization of a closed regenerative Brayton cycle for nuclear space power systems, Appl. Therm. Eng. 90 (2015) 250–257.
[14] M.C. Campos, J.V.C. Vargas, J.C. Ordonez, Thermodynamic optimization of a Stirling engine, Energy 44 (2012) 902–910.
[15] D.G. Thombare, S.K. Verma, Technological development in the Stirling cycle engines, Renew. Sustain. Energy Rev. 12 (2008) 1–38.
[16] R.J. Cassady, R.H. Frisbee, J.H. Gilland, M.G. Houts, M.R. LaPointe, C.M. Maresse-Reading, S.R. Oleson, J.E. Polk, D. Russell, A. Sengupta, Recent advances in nuclear powered electric propulsion for space exploration, Energy Convers. Manage 49 (2008) 412–435.
[17] M.S. El-Genk, J.-M. Tournier, A review of refractory metal alloys and mechanically alloyed-oxide dispersion strengthened steels for space nuclear power systems, J. Nucl. Mater. 340 (2005) 93–112.
[18] T. Liao, J. Lin, Optimum performance characteristics of a solar-driven Stirling heat engine system, Energy Convers. Manage 97 (2015) 20–25.
[19] M.H. Ahmadi, H. Sayyaadi, S. Dehghani, H. Hosseinzade, Designing a solar powered Stirling heat engine based on multiple criteria: maximized thermal efficiency and power, Energy Convers. Manage 75 (2013) 282–291.
[20] D. García, M.A. González, J.I. Prieto, S. Herrero, S. López, I. Mesonero, C. Villasante, Characterization of the power and efficiency of Stirling engine subsystems, Appl. Energy 121 (2014) 51–63.
[21] M. Babaelahi, H. Sayyaadi, A new thermal model based on polytropic numerical simulation of Stirling engines, Appl. Energy 141 (2015) 143–159.
[22] B. Kongtragool, S. Wongwises, A review of solar-powered Stirling engines and low temperature differential Stirling engines, Renew. Sustain. Energy Rev. 7 (2003) 131–154.
[23] L. Yaqi, H. Yaling, W. Weiwei, Optimization of solar-powered Stirling heat engine with finite-time thermodynamics, Renew. Energy 36 (2011) 421–427.
[24] S.C. Kaushik, S. Kumar, Finite time thermodynamic analysis of endoreversible Stirling heat engine with regenerative losses, Energy 25 (2000) 989–1003.
[25] Q. Yang, E. Luo, W. Dai, G. Yu, Thermoacoustic model of a modified free piston Stirling engine with a thermal buffer tube, Appl. Energy 90 (2012) 266–270.
[26] J. Ruelas, N. Velázquez, J. Cerezo, A mathematical model to develop a Scheffler-type solar concentrator coupled with a Stirling engine, Appl. Energy 101 (2013) 253–260.
[27] J.H. Shazly, A.Z. Hafez, E.T.E. Shenawy, M.B. Eteiba, Simulation, design and thermal analysis of a solar Stirling engine using MATLAB, Energy Convers. Manage 79 (2014) 626–639.
[28] W. Feng, C. Lingen, S. Fengrui, Y. Jiuyang, Performance Optimization of Stirling Engine and Cooler Based on Finite-Time Thermodynamic, Chemical Industry Press, Beijing, 2008.